Int. J. Solids Structures Vol. 29, No. 22, pp. 2761–2778, 1992
Printed in Great Britain

0020-7683/92 $5.00 + .00

MULTISCALE ROTATIONS IN DYNAMICALLY DEFORMED SOLIDS

YU. I. MESCHERYAKOV and S. A. ATROSHENKO
Institute of Machine Science, Academy of Science, Bolshoi 61, V.O., St Petersburg, 199178, Russia

(*Received* 18 *July* 1991; *in revised form* 15 *November* 1991)

Abstract—The conditions for realizing the rotation motion of material under shock loading are investigated by combining the laser interferometry of the free surface velocity and conventional methods of optical and electron microscopy. A detailed description of successive stages of the rotations forming both at the mesoscopical scale level and superstructural one is presented. It is shown that for realizing rotation motion at any scale level an essential difference is accelerations of adjacent microvolumes must be provided. The dimensionless ratio of the particle velocity distribution width to average particle velocity is suggested to be the criterion for change of the deforming and fracture mechanism from translational to rotational at some given scale.

NOMENCLATURE

$\bar{U}_{fs}$	average free surface velocity
ΔU_{fs}	free surface velocity distribution width
m	dynamical viscosity of the material
L	space dimension of the turbulence
r	mass density
$\Delta U_p = 1/2\Delta U_{fs}$	particle velocity distribution width at the mesolevel
d	diameter of rotations.

1. INTRODUCTION

Microscopic rotations in solids are now considered to be one of the ways in which the material responds to a non-uniform stress field. For quasi-static strain rates the rotation motion of media can be observed *in situ* by means of a speckle-technique (Panin *et al.*, 1989). However, the material's rotations during shock loading have not yet been studied because of the well-known experimental difficulties related to high-rate processes. Nevertheless, the dynamic rotation of material is thought to play an important role as an effective mechanism of energy dissipation and natural mechanism of transition from one scale level of deformation to another (Panin *et al.*, 1987). A suitable technique for studying the rotation motion of dynamically deformed and fractured materials was developed by C. M. Glass at 60th (Glass *et al.*, 1963). In his experiments a target of interest was cut along the wave propagation direction before shock loading and the microscopic network were plotted on the preliminary polished surfaces. Then both halves of the target were compacted back together, after shock loading the network lines were found to form different size circles.

In this work the main objective was to clarify the different situations in the shock loaded material for which rotation motion may be realized and to find correlations between particle velocity distributions at the several scale levels measured *in situ* by the laser interferometry technique (Asay and Barker, 1974; Divakov *et al.*, 1987) and the dimensions of the rotations measured by conventional methods of optical and electron microscopy.

2. EXPERIMENTAL APPROACH

Shock loading of the plane targets of different materials (copper, ductile steel, aluminium and its alloys, titanium) was carried out with a 27 mm bore diameter compressed-air gun. The impactor plates of the same material as the targets were mounted at the front of the projectile, which could be accelerated to the impact velocity 50–500 m s^{-1}. The

majority of the experiments were designed to include the material spallation in the later stages of the wave interaction process.

The free surface velocity histories were measured by using a velocity interferometer, the laser beam of which was focused to diameter 100–120 μm, which corresponds to the so-called superstructural scale level. According to Vladimirov (1987) this level corresponds to 2–10 grain sizes in polycrystals. This structural level is known to occupy an intermediate position between mesolevel (1–10 μm) (Vladimirov *et al.*, 1986) and macrolevel. Besides the time history at the level the interference method allows the particle velocity distribution width to be obtained (or the square root of the particle velocity dispersion) at the mesolevel by measuring the interference signal contrast (Asay and Barker, 1974; Divakov *et al.*, 1987).

At last, in a series of identical experiments with similar targets one can obtain the particle velocity distribution at the superstructural level, the average value of these data being equal to the macroscopic particle velocity.

For studying the rotation characteristics, especially for measurement of rotation angles, besides conventional optical and electron microscopy an original method of visualization of the rotations in deformed material based on the liquid crystal's properties was developed. All targets after shock loading were cut on one of the planes along the wave propagation direction and after polishing and etching a thin layer of liquid crystal was brought on the surface of interest. The liquid crystals are known to lay along the dense, compacted directions of monocrystal if the relevant conditions of moistening are provided. Looking at such prepared surfaces in polarized light one can see numerous round circles, the orientations of which are different in comparison with the rest of the crystal matrix. For early stages of rotation under small loading velocity, every rotation cell rotates as a solid, but with increasing loading velocity the interior of these circles is damaged, the separate fragments being considerably disoriented relative to each other.

3. EXPERIMENTAL RESULTS AND DISCUSSION

Results have been obtained using the techniques described above for a range of target materials, target thicknesses and flyer velocities. The qualitative picture of the plastic wave front configuration of two successive moments is shown in Fig. 1. This scheme shows that

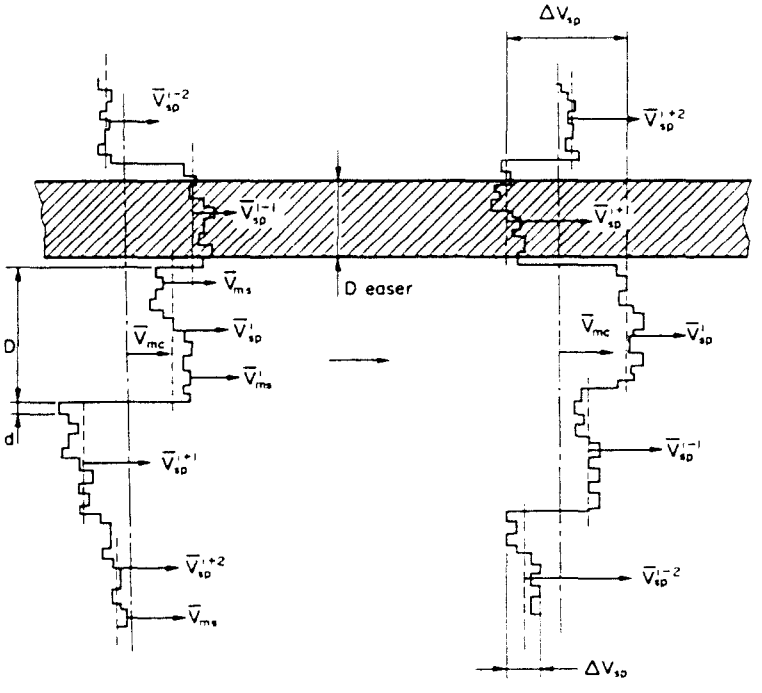

Fig. 1. Two instantaneous positions of the plastic front including the meso- and superstructural scale levels. The shaded band represents the laser interferometer beam dimension, which corresponds to the superstructural level.

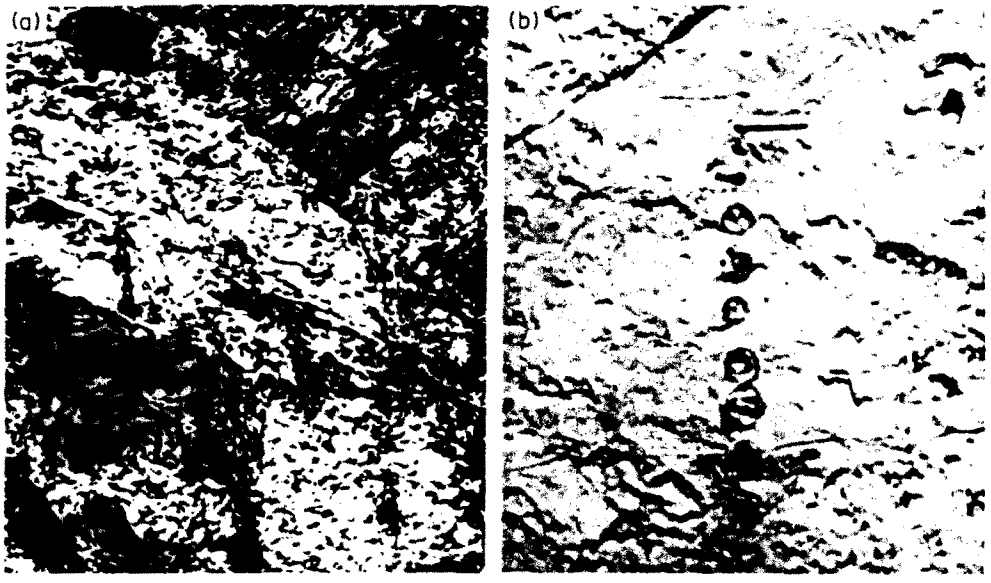

Fig. 2. Shear band in ductile steel (a) and rotation chain in copper (b) aligned along the wave propagation direction (indicated by arrow).

adjacent microvolumes continuously change their position relative to each other both at the mesolevel and superstructural level. As it turned out, depending on the ratio of the particle velocity distribution width (PVDW) to the average particle velocity the character of media motion in the shock compressed state may be essentially different. So when these values are comparable, when $\Delta V/V = 1$ the relative velocity of adjacent microvolumes is sufficient to provide a non-crystallographic shear banding in the wave propagation direction. One example of similar shear banding in ductile Cr-Bi-Mo steel is shown in Fig. 2a.

With the decrease in the PVDW when the ratio $\Delta V/V$ is approximately equal to a half, the material between adjacent microvolumes has time to rotate, the chains of rotations being aligned in the wave propagation direction as well as the shear bands. An example of the chain of rotations in copper is presented in Fig. 2b. It should be noted that the diameter of rotations in this figure changes non-monotonously along the chain reaching its maximum value twice. On the contrary, at the onset, in the middle and at the end of the chain the rotation diameter decreases. An average length of chains ranges within 50–180 μm, which corresponds to the space dimension of the plastic front. Indeed, for plastic wave velocity in copper 3.9 km s^{-1} and rise time of the plastic front 40 ns corresponding to the impact velocity 180 m s^{-1} one obtains the space dimension of the plastic front 160 μm.

Figure 3 shows a representative result for a copper target and the principal features associated with the stochastic behaviour of mesovolumes are clearly visible. Besides the interference signal and velocity profiles a time history of the PVDW are presented together.

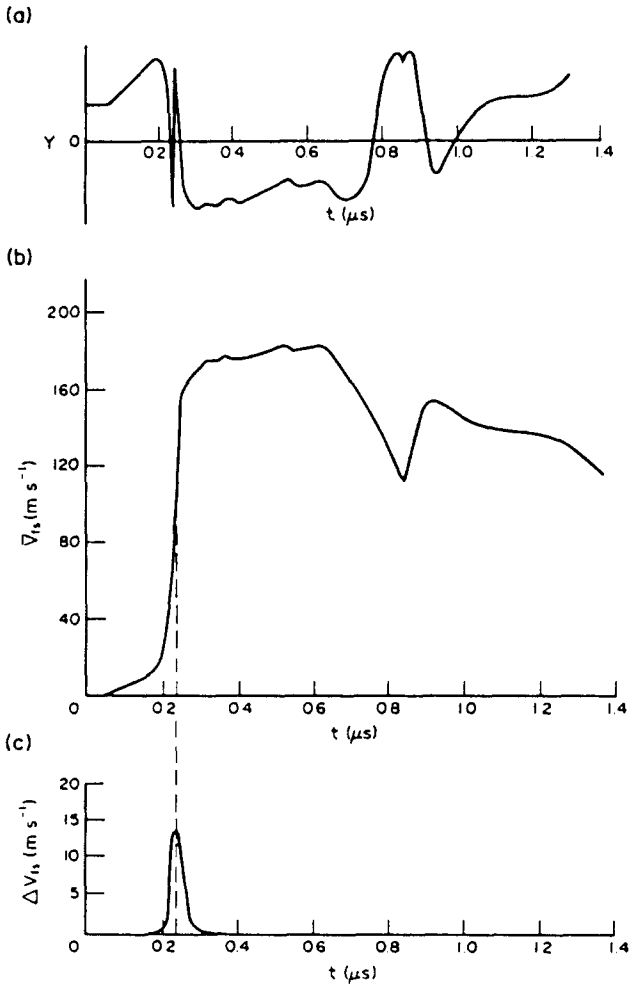

Fig. 3. Interferogram (a), free surface velocity profile (b) and free surface velocity disribution width (c) of copper M-3 loaded under flyer velocity 180 m s^{-1}.

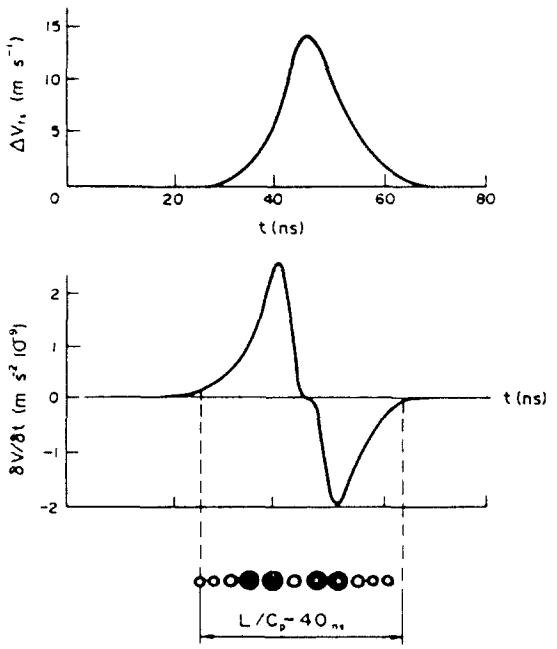

Fig. 4. Time profiles of the free surface velocity distribution width (a) acceleration (b) and rotation chain of copper.

It is seen that at the middle of the plastic front the PVDW reaches is maximum value that is inherent to the steady waves only. In such waves the particle velocity distribution has time to relax, narrowing after previously broadening during the first half of the plastic front. It suggests that the particles feel some acceleration at the first half of the wave front and deceleration at the second half. A separate time dependence of the particle acceleration of this free surface plastic front is shown in Fig. 4. One can see that the latter has two extremums which correspond to maximums of the rotations diameter (see at the bottom of this figure). This coincidence means that for rotation motion of the material the difference in the accelerations of microvolumes must be provided, that is the difference in the velocities of adjacent microvolumes must continuously change. On the other hand, the constant difference in velocities results in the shear banding. This conclusion is thought to be quite important for designing the adequate theoretical model of dynamic deformation and fracture.

A microscopic investigation shows that rotations of maximal sizes are as a rule damaged whilst the extreme and central rotation of small diameter are not damaged, the interior of undamaged rotations being surrounded by a thin round split. A detailed spectral analysis of the interior of these rotations was carried out by using a "Link" spectroscopic apparatus. In distinction from Christy *et al.* (1985) the presence of the second phase or any impurities was not found inside these cells. That is, their spectral composition turned out to be the same as that of the rest of the crystal matrix. All the data of the spectral analysis of copper M-2 are presented in Table 1.

Table 1.

Element	Atom per cent in matrix	Atom per cent inside cells
Cu K	99.186	99.333
Si K	0.230	0.000
P K	0.117	0.032
S K	0.079	0.000
Cl K	0.040	0.297
Ca K	0.069	0.009
Ti K	0.116	0.060
Ag L	0.059	0.060
Pb L	0.046	0.000

The second interesting example of the rotation motion of the solid under dynamic compression is presented in Fig. 5 where two steel targets loaded under different impact velocities revealed the opposite character of the relative motion of adjacent microvolumes along the wave propagation direction. On the left of them the relic bands of the material's rolling are shifted after shock loading in such a way that the same rolling bands belonging to different sides of the shear band can be connected as is shown by the dotted line (see Fig. 5a). However, this operation cannot be performed simultaneously on the right hand figure. The only possibility to explain the unusual curvature of rolling bands is to suggest the existence of the small rotations between microvolumes as is shown at the bottom of Fig. 5b. Later, these rotations were discovered by scanning microscopy. Their average size is measured to be 3–5 μm while the general displacement of opposite rolling bands relative to each other amounts to the value of 30 μm. From here the number of rotations covering this distance is estimated to be $n = L/nd = 2$ and every one of them had been rotated twice.

The next important aspect of the rotation motion of material in the shock waves is thought to be their unusual spherical form although one might expect that the relative motion of two adjacent microvolumes would only form cylindrical rotations. Nevertheless, the conclusion for the spherical form of rotations follows from the fact that their relic traces on the numerous random cuts of the targets are always round independent of the orientation of these cuts to the free surface of the targets. It permits us to suggest that the rotation motion is a result of non-uniform translational motion of three or more microvolumes, their relative velocities being changed to provide a non-zero difference in their accelerations in three-dimensional space.

It need hardly be said that the state of the solid during shock loading differs significantly from that of the unloaded material. According to modern theoretical and experimental data (Panin, 1987) the shock loading of a solid results in a transition into the so-called unstable structure state, which permits one to consider it as a viscous fluid. Experimental data on the local particle velocity disribution obtained *in situ* using the velocity interferometry allows us to estimate the local viscosity of the solid during rotation. The aforementioned whirl-like motion of dynamically loaded solids reminds one of analogous processes in the mechanics of fluids. The transition of media from laminar to turbulent motion is known to result in lowering the resistivity of viscous media. The flow regime depends on the relative velocities of adjacent flows ΔV, turbulent scale L, viscosity m, mass density r and can be characterized by the dimensionless value called Reynolds' number (Hintz, 1963): $Re = rL\Delta B/m$.

According to turbulence theory the inertial forces are known to be balanced by the viscous ones under a certain correlation between the previously numerated parameters. In but with increasing loading velocity the interior of these circles is damaged, the separate this case the energy exchange between microvolumes of media separated by the whirls can be neglected (the so-called "universal Kolmogorov equilibrium state"). In this zone the turbulence does not depend on the external conditions and the Reynolds number ties the flow parameters so that $Re = 1$. The scale factor L can be determined directly from photomicrographs in Fig. 2a for copper. The average particle velocity distribution width of this case corrresponds to $\Delta V = 7$ m s^{-1}. Taking the scale dimension of rotations $L = 5$ μm one can obtain the local viscosity 5 Ps, which differs from the average value for the same material approximately by two orders of magnitude (Chhabildas and Asay, 1979). Thus the local viscosity of a dynamically loaded solid during rotation turns out to be a very small value although the average viscosity may be great enough.

All rotation chains described are realized in the direct compressive waves and are the result of a difference in positive accelerations of the microvolumes. Another important kind of rotation motion of a solid is realized in the contrary release waves. These rotations are discovered between loaded and spall surfaces of the target only. An example of similar "field" rotations is presented in Fig. 6 for copper M-3. Application of the fluid-crystal technique revealed their local rotation relative to the solid matrix to be approximately 60°. In this material the average size of rotations equals 40–70 μm, which corresponds to a larger scale level in comparison with the rotations in the previously described chains. In aluminium and copper the "field" rotations are uniscale. In particular, in copper M-2 inside one grain

of size 150–200 μm a number of rotations are contained, some of which cross the grain boundaries without changing their form. This means that during rotation the material was in the unstable structure state for which the grain boundaries are not a sufficiently strong obstacle.

Microstructural investigations of shock loaded materials show that the development of the rotation motion is realized after exceeding a threshold. It suggests that below some critical value the localized deformation occurs along the crystallographic planes whose orientation is tangential to the future rotation cell (see Fig. 7). Thus, the future rotational cell turns out to be inside a polyhedron, the projection on the plane of cut appears as a circle inside a polygon.

The process of gradual evolution of new crystallographic planes of sliding oriented around the future rotation turns out to be observed on the single cut of a target using the so-called phenomenon of repeated spallation. The latter occurs when the tensile stress in the spall zone is essentially greater than critical spall strength. In this case the first wave decreased by the critical spall strength after first spallation remains sufficiently great for repeating the spallation at the new distance from free surface. Therefore, there may be several rows of spalling in one target. At each successive cross-section of the target, the value of the tensile stress being smaller than at the previous one, it is possible to observe the kinetics of development of the localized deformation or fracture including the kinetics of the gradual increase of the number of shear bands around the future rotation. Figure 8 shows how the picture of localized shear bands changes as one approaches the spall zone from a loaded surface. At the lower row the majority of the shear bands are oriented along the wave propagation direction but when the spall zone is approached the curvature of shear bands increases and at the last row the shear bands can be found to have a sharp break under the angle 60°. Lastly, the spall-split itself is a series of damaged disks inside polygons which are formed in turn by the crystallographic shear bands. From the picture presented one can see that by increasing the amplitude of the contrary release waves the curvature of the shear bands increases as well and after some threshold loading velocity the qualitative changing of the localization character occurs when a non-crystallographic mode of localized deformation in the form of rotation is realized.

For the ductile steel under investigation there are two kinds of rotational cells, the first corresponding to the mesolevel (3–7 μm) and the second to the superstructural level (60–200 μm). The successive stages of formation of the lower scale rotation are shown in Fig. 9. Before the central part of mesorotation begins to rotate an intensive fracture happens around the future rotation. This fracture results in the numerous fragments inside the narrow split surrounding the future rotation. However, until this split is locked the material inside the circle does not rotate. At the next stage shown in Fig. 9b the material begins to rotate, its fragments being gradually more round. During these stages a great deal of warmth is created by the rotation cell as a consequence of the friction and fragmentation processes occurring inside this cell. For the steel investigated an intensive heating of its interior causes a phase transition of martensite into ferrit around the rotational cell. The space range of this transition has a quite sharp front, as is clearly seen in Fig. 9a.

It was found that the transition of dynamically loaded solids into the rotational mode of deformation and fracture is accompanied by a sharp lowering of the amplitude of the shock impulse at the free surface of the target. For example, for the ductile steel investigated the free surface velocity at the impulse plateau decreases from 200 m s^{-1} to 150 m s^{-1}. This lowering is thought to be due to the aforementioned dissipative processes during rotation motion.

The second interesting mode of the rotation motion in solids at the mesolevel is presented in Fig. 10. Every mesorotation consists of a series of the plane fragments reminding one of a flower, the petals of it being slid relative to each other around a common centre. Thus, the mechanism of rotation motion in this case reduces to the plane sliding of fragments relative to each other, and translational motion of fragments to form the rotational motion of the mesovolume as a whole.

The individual mesorotations, in turn, can unite into chains, segments, spirals or circles depending on the particle velocity distribution at the superstructural scale level. Three

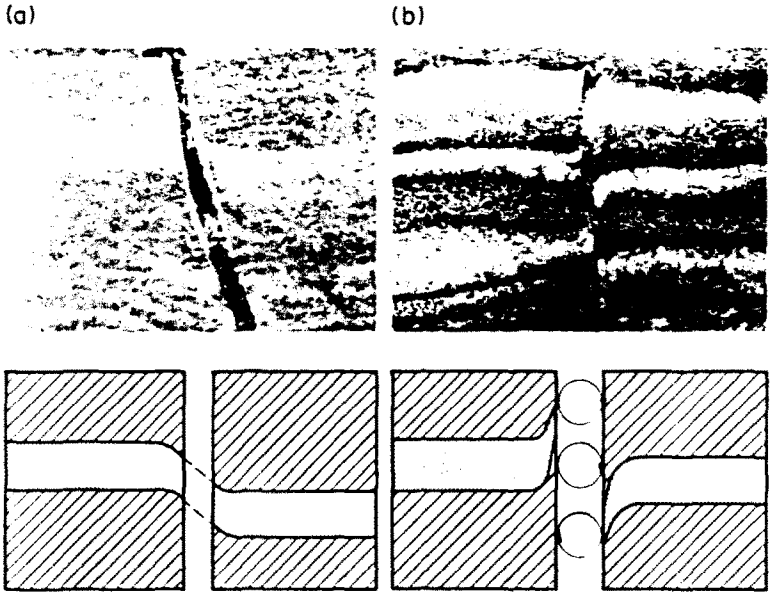

Fig. 5. Two different types of relative motion of adjacent microvolumes along the wave propagation direction: (a) shear banding, (b) rolling.

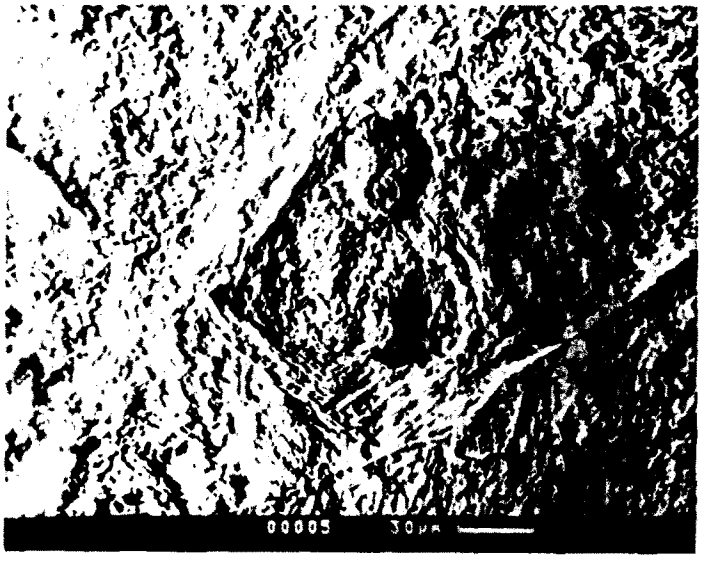

Fig. 6. "Field" rotations in copper.

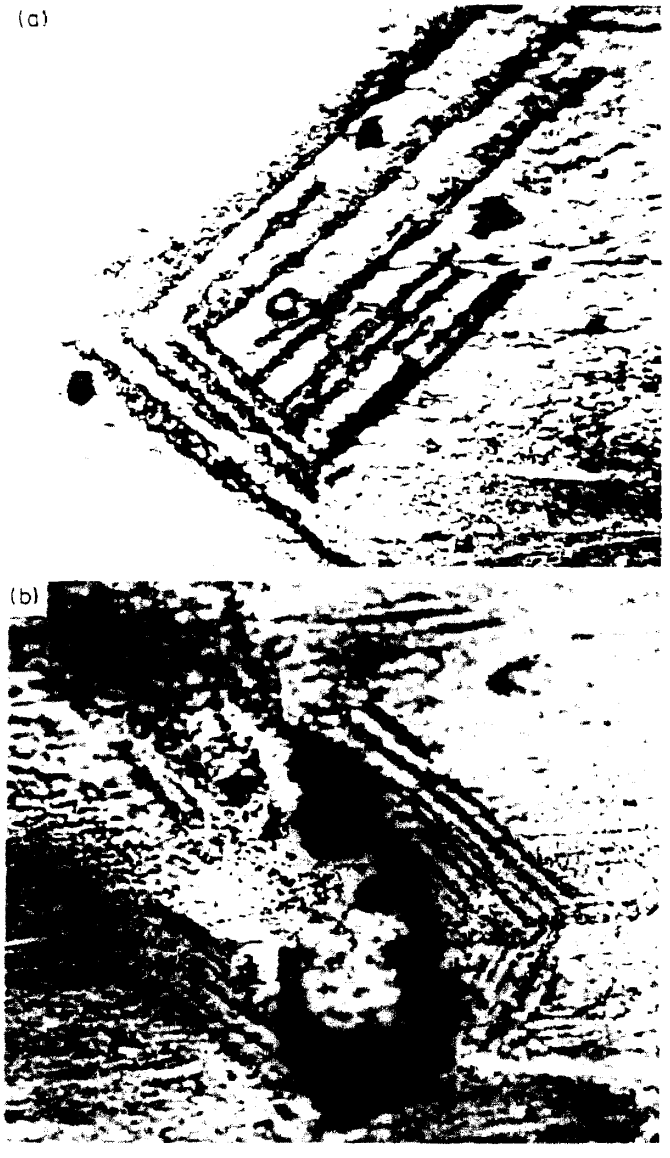

Fig. 7. Two successive stages of the field-rotations forming in copper: (a) shear banding around future rotation, (b) last stage of rotation when the round split is almost locked.

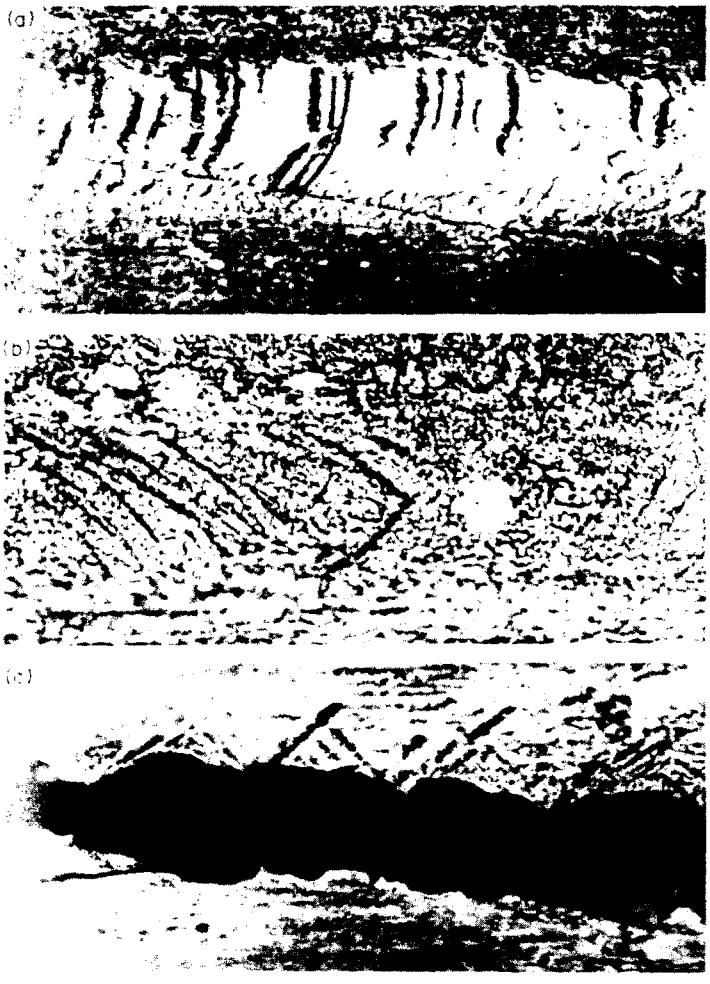

Fig. 8. Three successive stages of increasing the shear bands' curvature during repeated spalling. Upper photograph corresponds to perfect spall split formed by series of rotations.

Fig. 9. Two different possibilities for rotation forming in ductile steel: (a) and (b) undamaged interior of rotation, (c) damaged interior surrounded by the split with material's crumb.

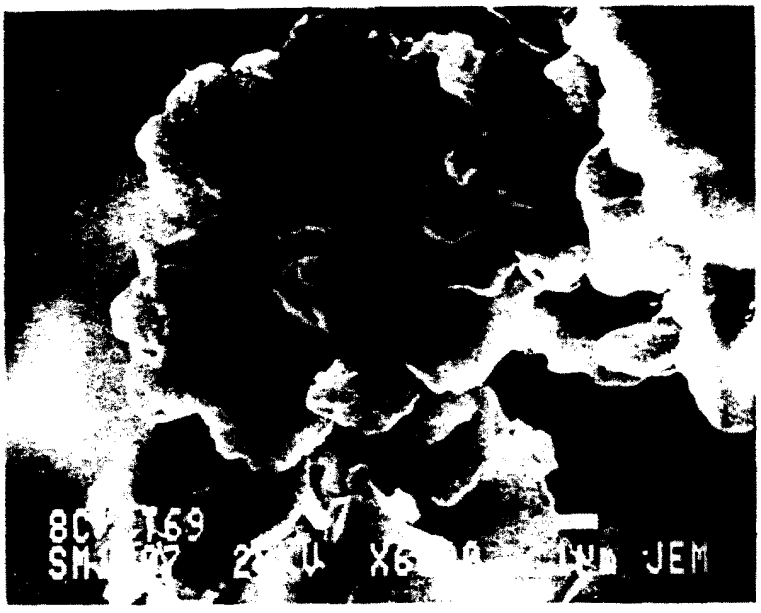

Fig. 10. Mesorotation in ductile steel consisting of plane fragments which move with a relatively common centre.

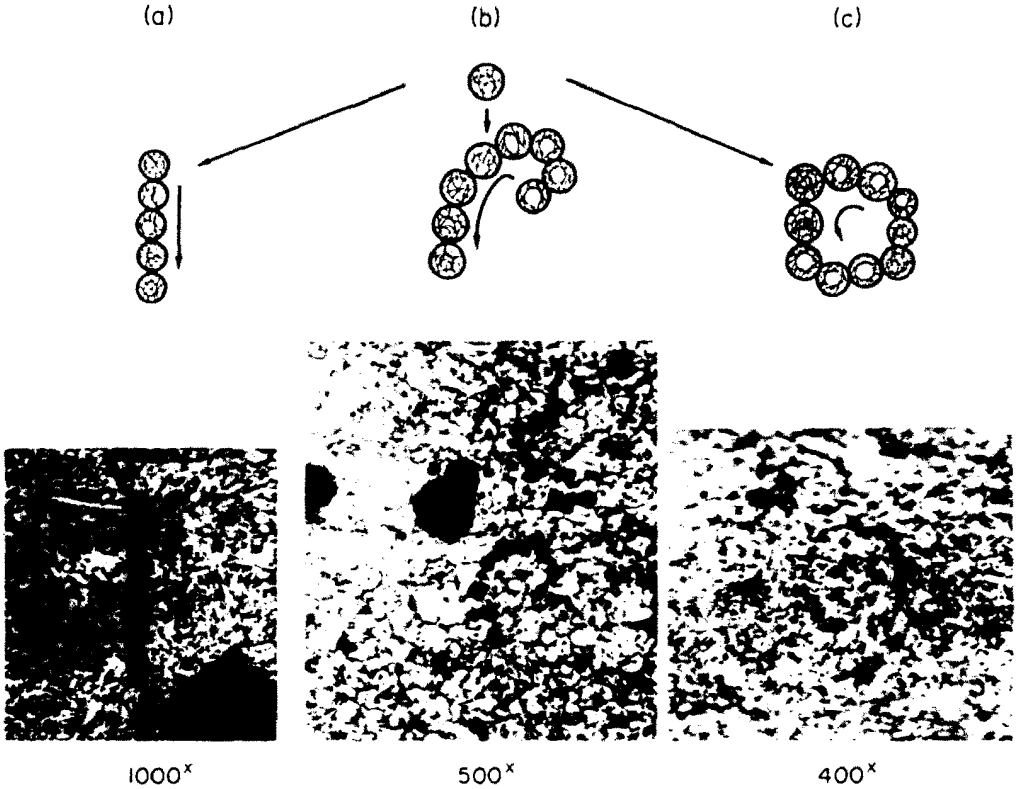

Fig. 11. Three ways of organizing the mesorotations into superstructural ones: (a) chain of mesorotations, (b) spiral, (c) circle. First and second ways correspond to the unsteady disribution at the superstructural level.

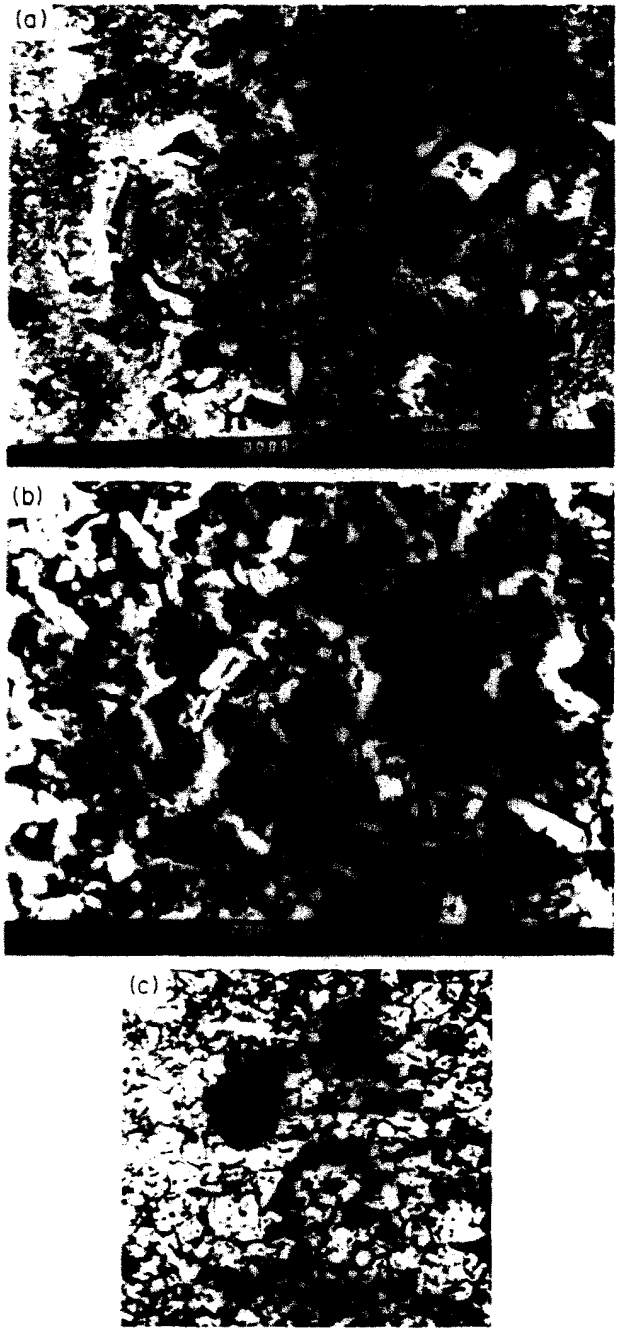

Fig. 12. Two successive stages of the rotation forming in aluminium alloy D-16.

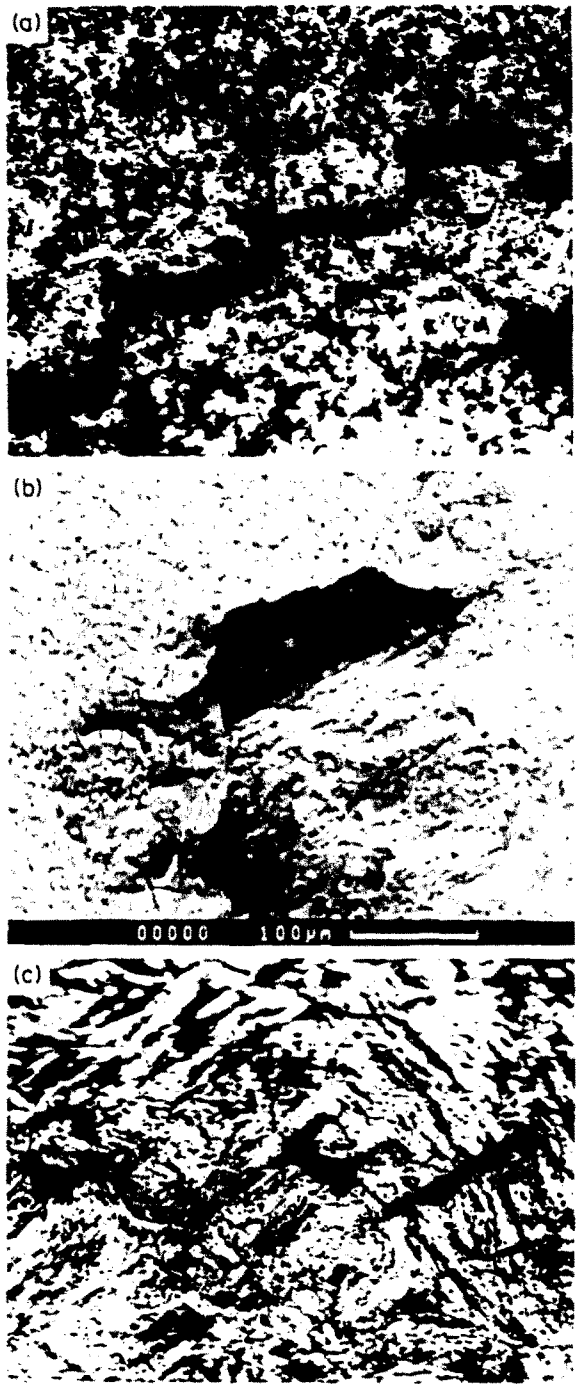

13. Three kinds of spall split depending on the ratio V/V: (a) step-like spall, (b) rotational spall split, (c) zigzag-like split.

Fig. 14. Two kinds of combined spall split (a) combination of the rotations at the mesolevel and translational damage at the superstructural scale level, (b) successive alternations of the rotation cells and the zigzag-like pieces in steel.

examples of these formations are shown in Fig. 11. It had been found before that the smaller the PVDW at the superstructural level the greater the rotation diameters at that level (Meshcheryakov *et al.*, 1989). For steady shock waves, super-rotations look like a perfect circle reminiscent of a "bearing", the interior of which rolls relative to the matrix by means of mesorotations. On the other hand, if the PVDW at that level changes during the impulse front, the radius of super-rotations changes as well. For example, the widening spiral shown in Fig. 11b corresponds to the narrowing of the particle velocity distribution at the superstructural level.

Thus, the main principle of forming the super-rotations is the same as that of meso-rotations. At the beginning of this process the mesorotations move around a future super-rotation and after the ring has been locked, the material inside begins to rotate, the distinct fragments being rotated relative to each other as well. This process is confirmed by the liquid crystal picture where the separate fragments inside the super-rotation are seen to be rotated at different angles.

The large-scale rotations at the superstructural level can be formed not only by the mesorotations but also by simple cracks. For aluminium alloy D-16, onset of the rotation is marked by the cracks disposed around and oriented in tangent directions to the circle. Two successive stages of forming the similar "brittle" rotation are shown in Fig. 12.

Finally, the spall zone itself can be formed by the rotation of one or another scale level depending on the particle velocity disribution at these levels. The dimensionless ratio $\Delta V/V$ can serve as a criterion for the transition from one to another mechanism of localized fracture. As it is seen from Fig. 13 the translational mechanisms are realized when that ratio tends to unity and the relative velocities of adjacent microvolumes are comparable with their average velocity. The spall-split of such material has a step-like form, a typical representative of which is shown in Fig. 13a.

Another extreme situation corresponds to the smallest value of the PVDW. In this case the difference in velocities of adjacent microvolumes is negligible so the material can be considered as isotropic and uniform. In the mechanics of solids the deformation of similar material is know to occur along the planes of maximal tangent directions that are at 45° relative to the wave propagation direction. Accordingly, the spall-split in such material has a zigzag-like form (see Fig. 13c). An intermediate position occupies the rotation way of spalling for which $\Delta V/V = 0.5$.

It should be noted that these criteria are thought to be correct both at the meso- and superstructural scale level. Furthermore, there are different combinations of mechanisms described, two of which are shown in Fig. 14. The first shows the piece of two-level spall-split, the failure of material at the mesolevel being realized by means of the rotation but at the superstructural level—by means of the shear banding. Another visible combination presented includes successive alterations of rotations and shear bands.

All mechanisms described are analysed here from the point of view of mechanical characteristics of the material such as an average particle velocity, a particle velocity distribution, stress and strain. The special interest in obtaining new materials concerns the metallurgical aspects of these mechanisms. Similar work was carried out by using a ductile steel of three regimes of tempering in order to provide the different microstructural and mechanical properties. Results of these investigations are now in preparation.

Acknowledgements—The authors wish to thank Drs A. K. Divakov, V. B. Vasilkov, A. I. Chernyshenko and Yu. A. Petrov for the performance of shock loading of materials and E. L. Aero and A. A. Shepelevsky for suggesting the fluid crystal technique of the rotation measuring. They also wish to thank Dr G. V. Kotov for making the JEM-micrographs of some materials.

REFERENCES

Asay, J. and Barker, L. (1974). Interferometric measurement. *J. Appl. Phys.* **45**, N6, 2545–2550.

Chhabildas, L. and Asay, J. (1979). Risetime measurement. *J. Appl. Phys.* **50**, N4, 2749–2756.

Christy, S., Pak, H. and Meyers, M. (1985). Effect of metallurgical parameters. In *Metallurgical Applications of Shock Waves and High-Strain-Rate Phenomena* (Edited by M. A. Meyers, L. E. Murr and K. P. Standhummer). EXPLOMET-85, 835–866.

Divakov, A., Kohanchik, L., Meshcheryakov, Yu. and Myshlyaev, M. (1987). To micromechanics of dynamic. *J. Appl. Mech. Techn. Phys.* **3**, 135–145.

Glass C. *et al* (1963). Symposium ASTM Dynamic Behavior Materials. Technical Publication No. 336.
Hintze, N. O. (1963). Turbulentnost. Physmagis.
Meshcheryakov, Yu., Atroshenko, S. and Divakov, A. (1989). Role of shock-induced particle. In *Shock Copmpression of Condense Matter* (Edited by S. C. Schmidt and J. N. Johnson), APS-3, p. 449. Elsevier, Amsterdam.
Panin, V., Zuev, L., Danilov and V. Mnikh, N. (1989). Plastic deformation. *DAN USSR* **308** (6). *Physics*, **1**, 34–54
Panin, V. E. Grinyaev, Yu. V. and Egoruskin, V. E. (1987). Spectrum of exciting states. *Izvestija VUZ'ov Physics*, **1**, 43–57.
Vladimirov, V. I. (1987). Cooperative effects. In *Questions of the Theory of Defects in Crystals*, pp. 43–57. Leningrad Science.
Vladimirov, V. I., Invanov, V. N. and Priemsky, N. D. (1986). Mesolevel of plastic deformation. In *Physics of Strength and Plasticity* (Edited by V. I. Vladimirov), pp. 69–80. Leningrad Science.